

# INTERACTING PION PAIRS IN NUCLEAR MATTER

N. GRION

*Istituto Nazionale di Fisica Nucleare, 34127 Trieste, Italy*

The CHAOS Collaboration

## Abstract

The pion-production  $\pi^+A \rightarrow \pi^+\pi^\pm A'$  reactions were studied on nuclei  ${}^2H$ ,  ${}^{12}C$ ,  ${}^{40}Ca$  and  ${}^{208}Pb$  at a pion energy of  $T_{\pi^+}=283$  MeV using the CHAOS spectrometer. The experimental results are reduced to differential cross sections and compared to both theoretical predictions and reaction phase space. Near the  $2m_\pi$  threshold pion pairs couple to  $(\pi\pi)_{I=J=0}$  when produced in the  $\pi^+ \rightarrow \pi^+\pi^-$  reaction channel. The  $\mathcal{C}_{\pi\pi}^A$  ratio between the  $\pi^+\pi^\pm$  invariant masses on nuclei and on the nucleon is also presented. The marked near-threshold enhancement of  $\mathcal{C}_{\pi^+\pi^-}^A$  is consistent with theoretical predictions addressing the partial restoration of chiral symmetry. On the opposite, nuclear matter weakly influences  $\mathcal{C}_{\pi^+\pi^+}^A$ .

## 1 Introduction

The influence of the nuclear medium on the  $\pi\pi$  interaction was studied at TRIUMF by means of the pion induced pion-production reaction  $\pi^+A \rightarrow \pi^+\pi^\pm A'$  (henceforth labelled  $\pi 2\pi$ ). The initial study was directed to the deuterium, to understand the  $\pi 2\pi$  behaviour on both a neutron and a proton then on complex nuclei  ${}^{12}C$ ,  ${}^{40}Ca$  and  ${}^{208}Pb$  to derive possible  $\pi\pi$  medium modifications by direct comparison of the  $\pi 2\pi$  data.

Early  $\pi 2\pi$  measurements[1] found that the near-threshold behaviour of the  $\pi^+\pi^-$  invariant mass  $M_{\pi^+\pi^-}^A$  increasingly peak toward the  $2m_\pi$  threshold as the nucleus mass number increases. Such a behaviour was explained by a theoretical approach of [2] which considered a  $\pi\pi$  pair a strongly interacting system when coupled to the  $I=J=0$  quantum numbers. The theory studies the  $(\pi\pi)_{I=J=0}$  properties in nuclear matter by dressing the single-pion propagator to account for the  $P$ -wave coupling of pions to  $p-h$  and  $\Delta-h$  configurations. The model is able to explain the general features of the  $M_{\pi^+\pi^-}^A$  distributions, which are predicted to increasingly accumulate strength near the  $2m_\pi$  threshold for  $\rho$ , the nuclear medium density, approaching  $\rho_0$ , the saturation density. Within the same theoretical framework, however, the near-threshold strength of the  $\pi\pi$   $T$ -matrix is considerably reduced when the  $\pi\pi$  interaction is constrained to be chiral symmetric[3], which may indicate that effects other than the in-medium  $(\pi\pi)_{I=J=0}$  interaction contribute to the observed strength. Conversely,

the absence of any in-medium modification of the  $(\pi\pi)_{I=J=0}$  interaction leads to  $M_{\pi^+\pi^-}^A$  distributions which lack of strength at threshold[1, 4]. In recent theoretical works on the  $(\pi\pi)_{I=J=0}$  interaction in nuclear matter[5], the effects of standard many-body correlations are combined with those deriving from the restoration of chiral symmetry in nuclear matter. As a result, the  $M_{\pi^+\pi^-}^A$  distributions are shown to regain strength near the  $2m_\pi$  threshold as  $A$  (thus the average  $\rho$ ) increases. Such a property was earlier outlined in some theoretical works, which demonstrated that the  $M_{\pi^+\pi^-}^A$  enhancement near threshold is a distinct consequence of the partial restoration of the chiral symmetry at  $\rho < \rho_0$  [6]. The purpose of this contribution is to present a set of  $\pi 2\pi$  data and to discuss it to the light of the most recent theoretical findings.

## 2 The experiment

The experiment was carried out at TRIUMF. Incident pions were produced by the collision of 480 MeV protons on a 10 mm thick graphite target. The M11 pion beam line transported the 282.7 MeV pions to the final focus. Pion pairs were detected in coincidence to ensure an unique identification of the pion production process.

CHAOS is a magnetic spectrometer which was designed for the detection of multi-particle events in the medium-energy range [7]. The magnetic field is generated by a dipole whose pole tip has 95 cm in diameter. The magnet is capable of producing a field intensity up to 1.6 T with an uniformity of about 1%. The top side has a 12 cm bore at the centre for the insertion of targets. Fig. 1 illustrates a reconstructed  $\pi_i^+ \rightarrow \pi^+\pi^-p$  events on  $^{12}\text{C}$  and the geometrical disposition of the wire chambers (WC), the CHAOS first level trigger hardware (CFT) and the magnet return yokes in the corners. WC1 and WC2 are multiwire proportional chambers which are capable of handling rates exceeding  $5 \times 10^6$  particles/s for extended periods of time with high efficiency ( $\sim 95\%$ ). They have a cylindrical shape with a diameter of 22.8 cm and 45.8 cm, respectively. WC3 is a cylindrical drift chamber designed to operate in a magnetic field, the chamber diameter is 68.6 cm. The outermost chamber WC4 is a vector drift chamber 122.6 cm in diameter, which operates outside of the magnetic field of CHAOS. The segments of WC3 and WC4 which were crossed by the incident particle beam were turned off. The CFT hardware consists of three coaxial cylindrical layers of fast-counting detectors. The first two layers are NE110 plastic scintillators 0.3 cm and 1.2 cm thick, respectively.  $\Delta E1$  is 72 cm far from the magnet centre and spans a zenith angle of  $\pm 7^\circ$ ; thus, it defines the geometrical solid angle of CHAOS  $\Omega=1.5$  sr. The third layer is a SF5 lead-glass 12.5 cm thick, about 5 radiation lengths, which is used as

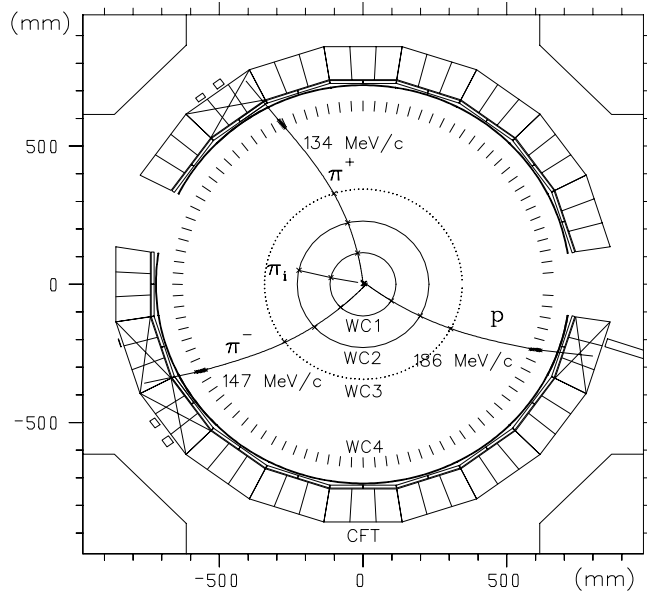


Figure 1: Reconstructed particle trajectories in CHAOS for the  $\pi_i^+ \rightarrow \pi^+ \pi^- p$  reaction on  $^{12}\text{C}$ , the geometrical disposition of the wire chambers (WC), the first level trigger hardware (CFT) and the magnet return yokes in the corners. Two CFT segments are removed to permit the particle beam ( $\pi_i$ ) to traverse the spectrometer. The CFT segments which are hit by particles are marked with crosses, and the energy deposited in  $\Delta E1$  and  $\Delta E2$  is indicated by boxes. The proton has a momentum slightly above the CHAOS threshold (185 MeV/c), and its energy is fully deposited in  $\Delta E1$ .

a Cerenkov counter. The three layers were segmented in order to provide an efficient triggering system to multi-particle events. Each segment covered an azimuthal angle (i.e., in-the-reaction plane) of  $18^\circ$ .

### 3 Analysis

The data reduction was based on fully reconstructed  $\pi^+ \rightarrow \pi^+ \pi^-$  and  $\pi^+ \rightarrow \pi^+ \pi^+$  events. In order to form differential cross sections these events were binned with their weights, which include the  $\pi^+ \pi^\pm$  decay rates inside CHAOS. The capability of the CHAOS spectrometer of measuring the kinetic energies ( $T$ ) and laboratory angles ( $\theta$ ) of each  $\pi \rightarrow \pi_1 \pi_2$  event permits the determination of the five-fold differential cross section  $\partial^5 \sigma / (\partial T \partial \Theta)_{\pi_1} (\partial T \partial \Theta)_{\pi_2} \partial \Phi_{\pi_1 \pi_2}$ , where  $\Phi_{\pi_1 \pi_2}$  is the zenithal angle between  $\pi_1$  and  $\pi_2$ , which CHAOS enabled measurement at both  $180^\circ \pm 7^\circ$  and  $0^\circ \pm 7^\circ$ . Four-fold differential cross sections were then obtained by integrating out the  $\Phi_{\pi\pi}$  dependence, which was performed by using a linear function joining the two measured data points. Such an assessment of the  $\Phi_{\pi\pi}$  dependence reflected in a systematic uncertainty of 8% ( $\sigma$ ) for the

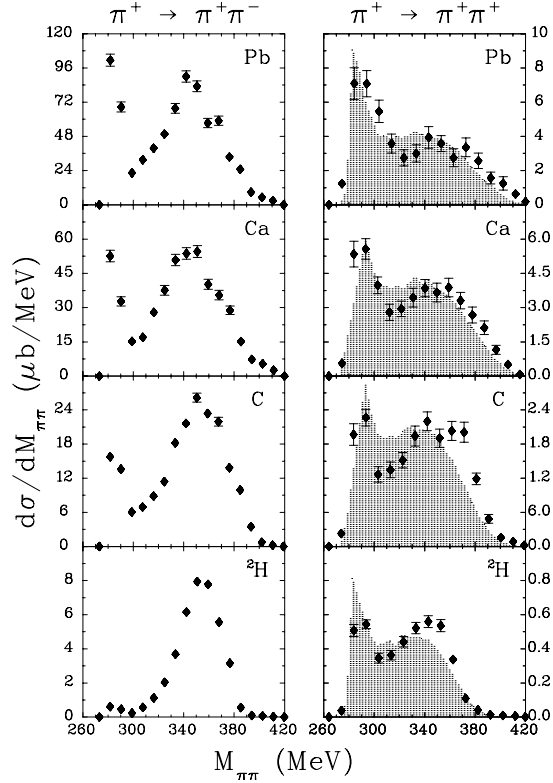


Figure 2: Invariant mass distributions (diamonds) for the  $\pi^+ \rightarrow \pi^+\pi^-$  and  $\pi^+ \rightarrow \pi^+\pi^+$  reactions on  ${}^2\text{H}$ ,  ${}^{12}\text{C}$ ,  ${}^{40}\text{Ca}$  and  ${}^{208}\text{Pb}$ . Diagrams (dots) are the result of phase-space simulations for the pion-production  $\pi A \rightarrow \pi\pi N[A-1]$  reaction.

deuterium and 6-7% ( $\sigma$ ) for nuclei. Furthermore, the data were reduced to single differential cross sections  $d\sigma/d\mathcal{O}_\pi$ , where  $\mathcal{O}_\pi$  represents  $(T_\pi$  or  $\Theta_\pi)_{1,2}$  or a combination of them. The cross section was then related to measured quantities  $\frac{d\sigma}{d\mathcal{O}_\pi} = f_e \frac{N(\mathcal{O}_\pi)}{\Delta\mathcal{O}_\pi}$ , where  $f_e$  is a parameter which is determined by the experimental conditions.

#### 4 Results of the $\pi \rightarrow \pi\pi$ reaction in nuclei

A general property of the  $\pi 2\pi$  process on nuclei in the low-energy  $M_{\pi\pi}$  regime was outlined by previous experimental works: it is a quasi-free process both when it occurs on deuterium [8] and on complex nuclei[9]. Furthermore, a common reaction mechanism underlies the process whether it occurs on a nucleon or a nucleus[10]. Thus the study of the  $\pi^+{}^2\text{H} \rightarrow \pi^+\pi^\pm NN$  reaction is dynamically equivalent to studying the elementary  $\pi^+n \rightarrow \pi^+\pi^-p$  and  $\pi^+p \rightarrow \pi^+\pi^+n$  reactions separately. In the present measurement, the  $\pi^+A \rightarrow \pi^+\pi^\pm A'$  reactions were studied under the same experimental conditions. Thus for a given

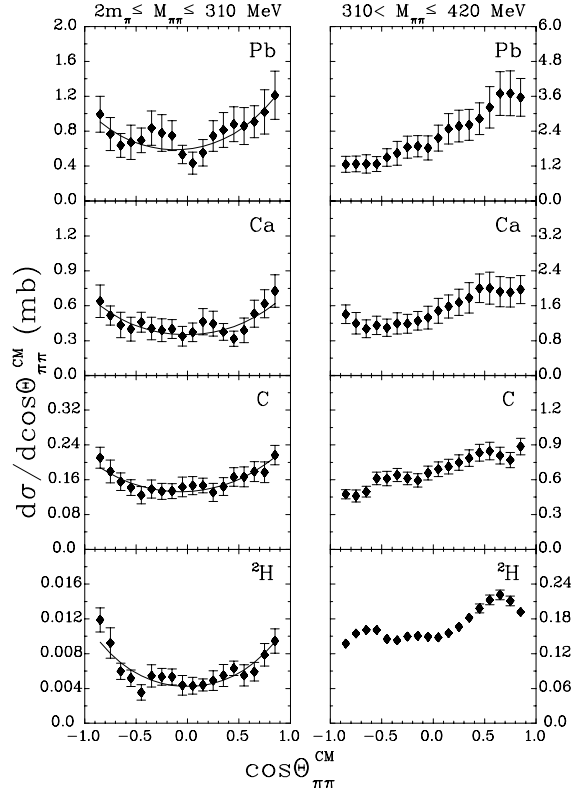


Figure 3: Distribution of the  $\cos\Theta$  in the  $\pi^+\pi^-$  centre-of-mass frame for the  $\pi^+A \rightarrow \pi^+\pi^-A'$  reaction at  $2m_\pi \leq M_{\pi\pi} \leq 310\text{MeV}$  (left frame), and at  $310 < M_{\pi\pi} \leq 420\text{MeV}$  (right frame). The solid lines are best-fit to the data including S, P and D waves.

observable the distributions are directly comparable. In addition, the moderate out-of-the-reaction plane angular acceptance of CHAOS may condition the intrinsic shape of the distributions. They are not corrected for it. The error bars explicitly reported on the spectra are the statistical uncertainties.

Fig. 2 shows the single differential cross sections (diamonds) as a function of the  $\pi\pi$  invariant mass ( $M_{\pi\pi}$ , MeV) for the two  $\pi^+ \rightarrow \pi^+\pi^-$  and  $\pi^+ \rightarrow \pi^+\pi^+$  reaction channels. The horizontal error bars are not indicated since they lie within symbols. The distributions span the energy interval available to the  $\pi\pi$  reaction which ranges from  $2m_\pi$ , the low-energy threshold, up the 420 MeV, the maximum allowed by the reaction. The  $\pi A \rightarrow \pi\pi N[A-1]$  phase space simulations (dotted histograms) are also provided and are normalized to the area subtended by the experimental distributions.

Regardless of the nucleus mass number, the invariant mass for the  $\pi^+ \rightarrow \pi^+\pi^+$  distributions closely follow phase space and the energy maximum increases

with the increase of  $A$ , that is, with the increase of the nuclear Fermi momentum. The  $\pi^+ \rightarrow \pi^+\pi^-$  channel discloses a different behaviour; as compared to phase space, the  ${}^2H$  invariant mass displays little strength from  $2m_\pi$  to 310 MeV while, on the same energy interval, the  ${}^{12}C$ ,  ${}^{40}Ca$  and  ${}^{208}Pb$   $\pi^+\pi^-$  invariant mass distributions increasingly peak as  $A$  increases.

In order to explain the nature of the reaction mechanism contributing to the peak structure, it is useful to examine the  $\cos\Theta_{\pi\pi}^{CM}$  distribution in the invariant mass interval of the peak, where  $\Theta_{\pi\pi}^{CM}$  is the angle between the direction of a final pion and the direction of the incoming pion beam in the  $\pi^+\pi^-$  rest frame. Fig. 3 shows the  $\cos\Theta_{\pi\pi}^{CM}$  distributions (diamonds) for  $2m_\pi \leq M_{\pi^+\pi^-} \leq 310$  MeV and  $310 < M_{\pi^+\pi^-} \leq 420$  MeV, the latter being shown for comparison. The vertical error bars are the overall uncertainties, which sum in quadrature the systematic and the statistic uncertainties. The differential cross sections are best-fitted (solid line) with a partial wave expansion limited to the three lowest waves, i.e. S, P and D. For all the studied nuclei is  $\chi_\nu^2 \leq 1$  which indicates that a proper number of waves was used in the expansion. In the case of heavier nuclei, the  $\pi^+\pi^-$  system predominantly couples  $S$ -wave  $\sim 95\%$  and a remaining 5% is spent in a  $D$ -wave state. Furthermore, within the sensitivity of the  $\chi_\nu^2$ -method any  $P$ -wave coupling of the two pions is excluded.

Two recent theoretical works [11, 12] have modelled the  $\pi 2\pi$  reaction on nuclei whose results are reported in Fig. 4. The (short and long) dashed lines denote the calculations of [11] while the results of the predictions are shown with the full lines [12]. In the case of  $Ca$ ,  $R1$  ( $R2$ ) indicates the predictions for  $\rho=0.7\rho_n$  ( $\rho=0.5\rho_n$ ), where  $\rho_n$  is the nuclear saturation density, while  $V1$  is the result of the calculations for a mean  $\rho=0.24\rho_n$ [13]. For both  ${}^2H$  and  ${}^{40}Ca$  the curves are normalized to the experimental data. For the  $\pi^+ \rightarrow \pi^+\pi^+$  channel, the predictions agree with the invariant mass distributions. The  $R1$  and  $R2$  distributions slightly differ from each other:  $R1$  presents a broader shape which is due to the larger nuclear Fermi momentum as a consequence of the higher nuclear density used[11]. The lower  $\rho$  used for  $R1$  seems to better fit the measured distribution, which is a trend also supported by  $V1$ . Therefore, both models and indicate that the average nuclear density of  ${}^{40}Ca$  for the production reaction to take place cannot exceed  $0.5\rho_n$ .

In the  $\pi^+ \rightarrow \pi^+\pi^-$  channel the distribution predicted by [12] for  ${}^2H$  is able to describe the data, although it tends to overestimate the low-energy  $M_{\pi\pi}$  yield. The present version of the model surely improves the previous versions[4], thus allowing for the construction of nuclear medium effects on a reliable ground. The approach of [12] includes several medium effects: Fermi motion, pion absorption,

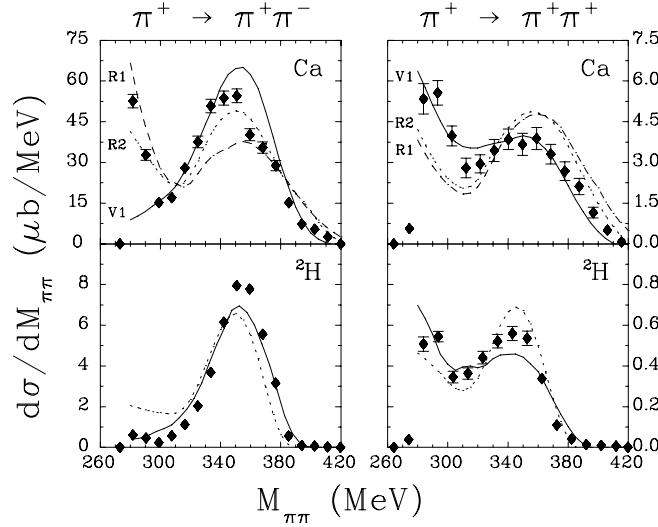


Figure 4: Invariant mass distributions (diamonds) for the  $\pi^+ \rightarrow \pi^+\pi^-$  and  $\pi^+ \rightarrow \pi^+\pi^+$  reactions on  ${}^2\text{H}$  and  ${}^{40}\text{Ca}$ . The dashed curves are taken from Ref.[11],  $R1$  and  $R2$  are the results for  $0.7\rho_n$  and  $0.5\rho_n$ , respectively. The full curves ( $V1$ ) are from the theoretical work of [12] for a mean density  $\rho=0.24\rho_n$ .

pion quasi-elastic scattering and  $(\pi\pi)_{I=J=0}$  medium modifications, which are able to reproduce only a moderate  $M_{\pi\pi}$  strength in the near-threshold region. In addition, an increase of  $\rho$  from  $0.24\rho_n$  to  $0.5\rho_n$  and to  $0.7\rho_n$  is unlikely to improve the agreement with the experimental cross section, see also Fig. 8 of Ref.[12]. In the case of[11], the  $R2$  prediction ( $0.5\rho_n$ ) seems to better reproduce the  $M_{\pi\pi}$  distribution, although some of the near threshold yield already derives from the the low-energy  $\pi^+ {}^2\text{H} \rightarrow \pi^+\pi^-pp$  production. Therefore,  $V1$ ,  $R1$  and  $R2$  suggest that the  $M_{\pi^+\pi^-}$  missing strength near the  $2m_\pi$  threshold should be searched in a stronger  $\rho$ -dependence of the  $(\pi\pi)_{I=J=0}$  interaction, rather than requiring an unlikely high-density nuclear environment for the pion-production process to occur.

The observable  $\mathcal{C}_{\pi\pi}^A$  is presented in comparison with recent theoretical predictions.  $\mathcal{C}_{\pi\pi}^A$  is defined as the composite ratio  $\frac{M_{\pi\pi}^A}{\sigma_T^A} / \frac{M_{\pi\pi}^N}{\sigma_T^N}$ , where  $\sigma_T^A$  ( $\sigma_T^N$ ) is the measured total cross section of the  $\pi 2\pi$  process in nuclei (nucleon). This observable has the property of yielding the net effect of nuclear matter on the  $(\pi\pi)_{I=J=0}$  interacting system regardless of the  $\pi 2\pi$  reaction mechanism used to produce the pion pair [10]. Therefore,  $\mathcal{C}_{\pi\pi}^A$  can be compared with the [11, 12] predictions which explicitly calculate both  $M_{\pi\pi}^{\text{Ca}}$  and  $M_{\pi\pi}^{{}^2\text{H}}$ , but also with the theories described in [5, 6] because they calculate the mass distribution of an interacting  $(\pi\pi)_{I=J=0}$  system both in vacuum and in nuclear matter. Since the

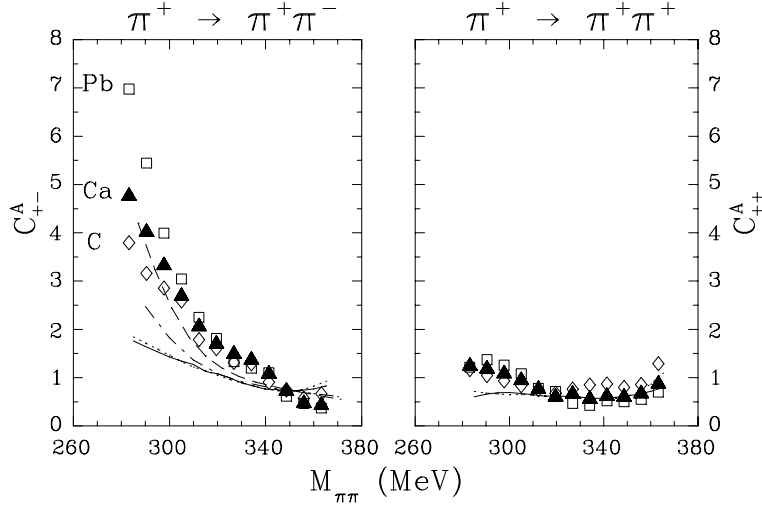


Figure 5: The composite ratios  $\mathcal{C}_{\pi\pi}^A$  for  $^{12}\text{C}$ ,  $^{40}\text{Ca}$  and  $^{208}\text{Pb}$ . The curves are taken from [12] (full), [11] (dotted), [6] (dash-dotted) and [5] (dashed). Further details are reported in the text.

above calculations are reported either in arbitrary units [11, 12] or in units which are complex to scale [5, 6], theoretical predictions are normalized to the experimental distributions at  $M_{\pi\pi}=350\pm 10$  MeV, where  $\mathcal{C}_{\pi\pi}^A$  presents a flat behaviour Fig. 5.

For both reaction channels, the full[12] and dotted [11] curves in Fig. 5 are obtained by simply dividing  $M_{\pi\pi}^{Ca} / M_{\pi\pi}^{2H}$ . Furthermore, for both approaches the underlying medium effect is the  $P$ -wave coupling of  $\pi$ 's to  $p-h$  and  $\Delta-h$  configurations, which accounts for the near-threshold enhancement. When applied to the  $\mathcal{C}_{\pi\pi}^{Ca}$ , both [11] and [12] predict the same result; in fact, they well describe the behaviour of  $\mathcal{C}_{++}^{Ca}$  throughout the  $M_{\pi\pi}$  energy range, while for  $\mathcal{C}_{+-}^{Ca}$  only part of the near-threshold strength is reproduced. The models of Refs. [5, 6] examine the medium modifications on the scalar-isoscalar meson, the  $\sigma$ -meson. Nuclear matter is assumed to partially restore chiral symmetry and consequently  $m_\sigma$  to vary with  $\rho$ , the variation being parametrised as  $1-p\frac{\rho}{\rho_n}$ , where  $p$  can range in the interval  $0.1 \leq p \leq 0.3$  for [6] and  $0.2 \leq p \leq 0.3$  for [5], and for both is  $\rho=\rho_n$ . Both models are capable of yielding large strength near the  $2m_\pi$  threshold, therefore the capability of predicting  $\mathcal{C}_{+-}^A$  is compared for a common minimum value of the parameter  $p=0.2$ . In Fig. 5 the predictions of [6] and [5] are reported with dash-dotted line and dashed line, respectively. The model [5] provides a larger near-threshold strength, which is due to the combined contributions of the in-medium  $P$ -wave coupling of pions to  $p-h$  and  $\Delta-h$  configurations and to the partial restoration of chiral symmetry in



nuclear matter. This model, however, is still too schematic for a conclusive comparison to the present data, therefore full theoretical calculations are called for.

## 5 Conclusions

$\mathcal{C}_{\pi\pi}^A$  was found to yield the net effect of nuclear matter on the  $\pi\pi$  system regardless of the  $\pi 2\pi$  reaction mechanism used to produce the pion pair. These distributions display a marked dependence on the charge state of the final pions: (i) the  $\mathcal{C}_{\pi^+\pi^-}^A$  distributions peak at the  $2m_\pi$  threshold and the yield increases as  $A$  increases thus denoting that pion pairs form a strongly interacting system; furthermore, the  $\pi\pi$  system couples to the  $I = J = 0$  channel, the  $\sigma$ -meson channel. (ii) In the  $\pi^+ \rightarrow \pi^+\pi^+$  channel, the  $\mathcal{C}_{\pi\pi}^A$  behaviour barely depends on both  $A$  and  $T$  thus indicating that nuclear matter weakly affect the  $(\pi\pi)_{I,J=2,0}$  interaction. The  $\mathcal{C}_{\pi^+\pi^-}^A$  observable was compared with theories studying the  $(\pi\pi)_{I=J=0}$  in-medium modifications associated to the partial restoration of chiral symmetry in nuclear matter, and with model calculations which only include standard many-body correlations, i.e. the  $P$ -wave coupling of  $\pi$ 's to  $p - h$  and  $\Delta - h$  configurations. It was found that both mechanisms are necessary to interpret the data, although chiral symmetry restoration yields the larger near-threshold contribution. Whether this conclusion is correct, the  $\pi 2\pi$  CHAOS data would indicate an example of a distinct  $QCD$  effect in low-energy nuclear physics.

Montecarlo simulations of the  $\pi^+ A \rightarrow \pi^+\pi^\pm N[A - 1]$  reaction phase space revealed useful to interpret some of the  $\pi 2\pi$  data. In the case of  $M_{\pi^+\pi^+}$ ,  $\pi^+\pi^+$  pairs distribute according to phase space. In addition, simulations are able to describe the high-energy part of the distributions which are sensitive to the nuclear Fermi momentum of the interacting  $\pi^+ p[A - 1] \rightarrow \pi^+\pi^+ n[A - 1]'$  proton. For the  $M_{\pi^+\pi^-}$  distributions the  $\pi\pi$  dynamics overwhelms the dipion kinematics: unlike phase space, the near-threshold  $\pi^+\pi^-$  yield is suppressed in the elementary production reaction,  $\pi^+ {}^2H \rightarrow \pi^+\pi^- pp$  in the present work, while in the same energy range medium modifications strongly enhance  $M_{\pi^+\pi^-}$ . A guideline to the interpretation of the  $M_{\pi^+\pi^\pm}^A$  behaviour should combine the effects of the chiral symmetry restoration in nuclear matter and standard many-body correlations. Such an approach would exclude high-density nuclear matter for both the production reaction to take place and the  $\pi\pi$  system to undergo medium modification.

## References

- [1] P. Camerini, N. Grion, R. Rui and D. Vetterli, Nucl. Phys. **A552**, 451 (1993).
- [2] P. Schuck W. Nörenberg and G. Chanfray, Z. Phys. **A330**, 119 (1988); G. Chanfray, Z. Aouissat, P. Schuck and W. Nörenberg, Phys. Lett. **B256**, 325 (1991).
- [3] Z. Aouissat R. Rapp, G. Chanfray, P. Schuck and J. Wambach, Nucl. Phys. **A581**, 471 (1995);
- [4] E. Oset and M. J. Vicente-Vacas, Nucl. Phys. **A454**, 637 (1986).
- [5] Z. Aouissat G. Chanfray, P. Schuck and J. Wambach, nucl-th/9908076 v2 31 Aug 1999.
- [6] T. Hatsuda, T. Kunihiro and H. Shimizu, Phys. Rev. Lett. **82** 2840(1999).
- [7] G.R. Smith *et al.*, Nucl. Instr. and Meth. in Phys. Res. **A362**, 349 (1995).
- [8] R. Rui et al., Nucl. Phys. **A517**, 445 (1990); V. Sossi et al., Nucl. Phys. **A548** 562 (1992).
- [9] F. Bonutti *et al.*, Phys. Rev. **C55**, 2998 (1997).
- [10] F. Bonutti *et al.*, Phys. Rev. **C60**, 018201(1999).
- [11] R. Rapp, J. W. Durso, Z. Aouissat G. Chanfray, O. Krehl, P. Schuck J. Speth and J. Wambach, Phys. Rev. **C59**, R1237 (1999).
- [12] M. J. Vicente-Vacas and E. Oset, Phys. Rev. **C60**, 064621(1999).
- [13] M. J. Vicente-Vacas and E.Oset, nucl-th/0002010 Feb. 2000.